A study of the molecular mechanism of action of Jiawei Guizhishaoyaozhimu Decoction during rheumatoid arthritis therapy based on basic of network pharmacology and experimental verification

YIJI CHENG[1], YUE JI[2], KAIDI FENG[2], XINYUAN ZHANG[2], YUNMING XIAO[3] and WEIXIA JING[1]

[1]Department of Rheumatology and Immunology, Beijing University Of Chinese Medicine Third Affiliated Hospital, Beijing 100029; [2]Graduate School, Tianjin University of Traditional Chinese Medicine, Tianjin 301617; [3]State Key Laboratory of Kidney Diseases, First Medical Center of Chinese People's Liberation Army General Hospital, Medical School of Chinese People's Liberation Army, Beijing 100000, P.R. China

Abstract. Rheumatoid arthritis (RA) is a chronic autoimmune disease, which primarily affects the joints. The aim of the present study was to predict the main active ingredients of Jiawei Guizhishaoyaozhimu Decoction (JWGZSYZMD) and potential targets of this treatment during RA therapy by using molecular docking and network pharmacology methods. In addition, another aim was to investigate the therapeutic effects and mechanism of JWGZSYZMD on joint inflammation in rat models of collagen II-induced arthritis (CIA). JWGZSYZMD ingredients and targets and genes associated with RA first extracted from traditional Chinese medicine (TCM) Systems Pharmacology Database and Analysis Platform, Bioinformatics Analysis Tool of Molecular Mechanism-TCM and Genecards databases, which were then transferred to the STRING database to set up protein interaction networks. The crystal structures of target proteins were also downloaded from the Protein Data Bank before molecular docking of compounds onto the protein targets was performed using AutoDock Vina software. In addition, a drug compound target visualization network was constructed using Cytoscape 3.7.2 software, which was used to elucidate the main mechanism underlying the anti-RA effect of JWGZSYZMD. A CIA rat model was established and animals were divided into the control, CIA model, JWGZSYZMD treatment (low-, medium- and high-dose) and tripterygium glycoside groups. Compared with the rats in the CIA model group, the joint scores of the rats in the high-dose group of JWGZSYZMD were significantly lower after 21 days of treatment. The expression levels of IL-6, TNF-α, IL-1β and IL-17A in the synovial supernatant of the model rats were lower compared with those in the CIA group. Also, the expression of the aforementioned cytokines in the high-dose JWGZSYZMD group was significantly lower compared with those in the CIA model group. To conclude, using molecular docking combined with network pharmacology, the material basis and molecular mechanism underlying the effects of JWGZSYZMD during RA therapy were studied, which could potentially provide a reference for future clinical applications.

Introduction

Guizhishaoyaozhimu Decoction (GSZD) has been used as a Traditional Chinese Medicine (TCM) since at least the Han Dynasty period, for >2,000 years in China. It has mainly been used for the treatment of anemofrigid-damp arthralgia (1). At present, it is commonly prescribed in clinical practice, particularly for the treatment of rheumatoid arthritis (RA) and other joint disease, such as osteoarthropathy (2). It has been previously reported to significantly alleviate pain and swelling in patients whilst effectively promoting the recovery of joint function (3). RA is an autoimmune disease with symmetrical, invasive swelling and pain in the small joints, such as the metacarpophalangeal joints (4). RA frequently affects multiple joints in the same individual (5,6). It has been reported that 0.5-1% of the global population is affected by RA (7). RA inflammation is associated with overproduction of inflammatory factors, expressing high levels of inflammatory factors, chemokines, and adhesion molecules (e.g., IL-6, TNF-α,

Correspondence to: Dr Weixia Jing, Department of Rheumatology and Immunology, Beijing University of Chinese Medicine Third Affiliated Hospital, 51 Anwaixiaoguan Road, Chaoyang, Beijing 100029, P.R. China
E-mail: apolline999@163.com

etc.)causing synovial inflammation (8). It also promotes the formation and maintenance of T and B cell survival and the formation of a specific immune microenvironment (9). Yan *et al* previously reported beneficial effects exerted by Jiawei Guizhishaoyaozhimu Decoction (JWGZSYZMD), which is based on the original GSZD preparation supplemented with 'Bu Gu Zhi' (*Fructus Psoraleae*) and 'Gu Sui Bu' (*Rhizoma Drynariae*). These compounds have previously been proposed as therapeutic agents for treating muscle and joint pain and stiffness, regardless of the disease location, size of the joint or the course of disease (10,11). In addition, the use of 'Sang Zhi' (*Ramulus Mori*) before the signs of arthritis-induced fever has been documented to confer beneficial effects clinically (12,13).

In the present study, 'Gu Sui Bu', 'Sang Zhi' and 'Bu Gu Zhi' were added into the existing formulation of GSZD. A collagen II-induced arthritis (CIA) model was established in rats to observe the efficacy of JWGZSYZMD on joint inflammation. In addition, its effects on IL-1, IL-6, IL-17 and TNF-α expression levels were measured. The aim of the present study was to interpret the effects and underlying mechanism of action of JWGZSYZMD in the treatment of RA, in addition to establishing an active component-disease target regulatory network to predict core targets for RA therapy.

Materials and methods

Network pharmacological study
Acquisition of targets corresponding to prescription. JWGZSYZMD was comprised of 'Gui Zhi' (*Ramulus Cinnamomi*), 'Bai Zhu' (*Rhizoma Atractylodis Macrocephalae*), 'Gan Cao' (Zhi; *Radix Glycyrrhizae Uralensis*), 'Ma Huang' (*Herba Ephedrae*), 'Bai Shao' (*Raidix Paeoniae Alba*), 'Zhi Mu' (*Rhizoma Anemarrhenae*), 'Sheng Jiang' (*Rhizoma Zingiberis Recens*), 'Fang Feng' (*Radix Saposhnikoviae*), 'Bu Gu Zhi' (*Fructus Psoraleae*), 'Fu Zi' (*Radix Aconiti Lateralis Preparata*), 'Sang Zhi' (*Ramulus Mori*) and 'Gu Sui Bu' (*Rhizoma Drynariae*) (Fig. 1). Traditional Chinese Medicine Systems Pharmacology Database and Analysis Platform (TCMSP; tcmsp-e.com/) was used to obtain ingredients and targets corresponding to these aforementioned compounds. 'Bu Gu Zhi' is not included in TCMSP and was instead analyzed using the Bioinformatics Analysis Tool of Molecular Mechanism of Traditional Chinese Medicine (BATMAN-TCM, http://bionet. ncpsb.org.cn/batman-tcm/index.php/Home/Index/index) to obtain the ingredients and targets. Orally-applied TCM has to overcome the obstacles of the absorption, distribution, metabolism and excretion process for maximal efficacy, in which oral bioavailability (OB) is an important pharmacokinetic parameters. Substances with OB value ≥30% were considered to have a high OB. Drug-likeness (DL) was used to estimate the pharmacological properties of molecules and is useful for the rapid screening of active substances. It has been previously reported that substances with DL ≥0.18 would indicate a superior effect (14). Therefore, the screening criteria for active ingredients in the present study were OB ≥30% and DL ≥0.18 in the TCMSP database, whereas in BATMAN-TCM the screening criteria were score ≥20 and P<0.05 (15,16).

Acquisition of RA-associated drug targets. The corresponding genes associated with RA were obtained from the

Genecards database (https://www.genecards.org/) using the term 'Rheumatoid Arthritis' (17). The potential drug targets were mapped against the genes corresponding to RA to obtain potential mechanisms by which JWGZSYZMD regulated RA.

Construction of the drug-active component-target regulatory network. Corresponding drug-active component-target regulatory networks were constructed using the Cytoscape 3.7.2 software (cytoscape.org). Possible connections between drug composition and active ingredients of JWGZSYZMD, in addition to their potential regulatory targets in the context of RA, were then visualized. According to the number of connecting nodes and determination of the core based on network topology parameters targets and the main active ingredients that exert pharmacological effects, the potential active ingredients contained within the JWGZSYZMD for regulating RA were screened.

Protein-protein interaction (PPI) for predicting the core target of JWGZSYZMD in the treatment of RA. Relationships among the targets of JWGZSYZMD in RA were then assessed using the STRING database (https://cn.string-db.org/), where targets ranked in the top 30 in terms of the number of connections were visualized using histograms (18). In addition, a network representing the specific relationships among the targets were visualized using the Cytoscape software (18).

Path prediction of JWGZSYZMD in the treatment of RA. Targets of JWGZSYZMD predicted to regulate RA were screened for in Kyoto Encyclopedia of Genes and Genomes (KEGG) pathways using the STRING database, with the criteria of P<0.05 (19). The top 10 ranked KEGG pathways were then visualized using bubble plots after selecting the RA-related pathways.

Molecular docking. In summary, 3D structures of IL-1β, IL-6, IL-17A and TNF-α targets were retrieved from the Protein Data Bank (PDB) protein structure database (http://www.rcsb.org/). The structures were then saved in the '.pdb' format after using the PyMol 2.4 (pymol.org/2) software to delete water molecules and small molecule ligands. Using the Pubchem database (http://zinc.docking.org/), 2D structures of the top 30 ranked active ingredients were retrieved, before their minimum free energies were calculated using Chem3D 6.6.0 (chemdoodle.com/3d/) software and saved in the 'MOL2' format. The aforementioned active ingredients and targets were then input into AutoDockTools 1.5.6 (autodock.scripps.edu) software for hydrogenation and format conversion, before being output into the 'PDBQT' format. Previous studies have reported that the involvement of TNF-α and IL-6 forms the core of RA pathogenesis (20,21). However, IL-6 is also a regulatory factor in bone metabolism, in which IL-17 and IL-1β also serve an important role (20,21). Therefore, AutoDock Vina 1.1.2 (vina.scripps.edu) was used to perform molecular docking for TNF-α, IL-6, IL-17 and IL-1β, where the minimum binding energy of each potential active ingredient onto each of these proteins was calculated. The three results which demonstrated the most optimal molecular docking visualized using PyMol and Ligplot 2.2 (ebi.ac.uk/thornton-srv/software/LIGPLOT) software.

Experimental validation studies
Experimental reagents. Bovine collagen II (cat. no. 20022; Chondrex, Inc.), Freund's incomplete adjuvant (cat. no. 7002;
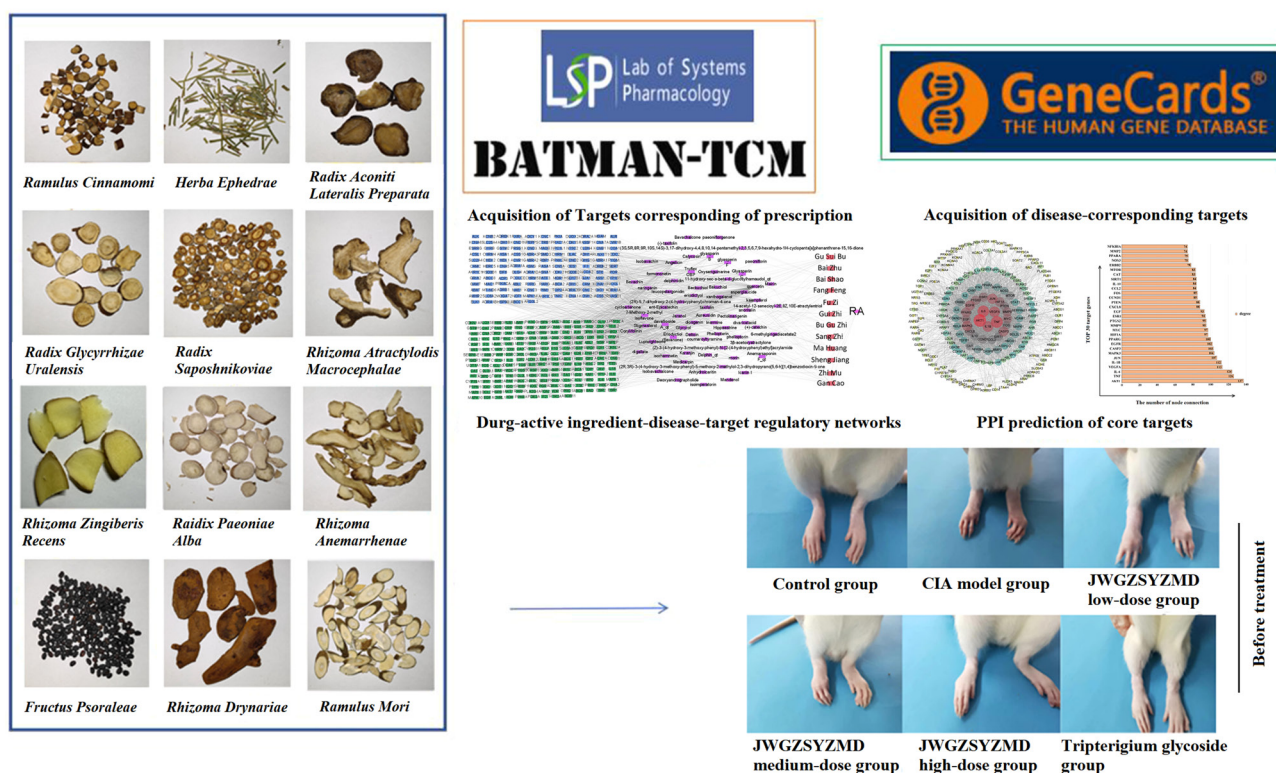
Figure 1. Flow diagram of the research design in the present study and images of rats are representative of the rate in each group. CIA, collagen II-induced arthritis; BATMAN-TCM, Bioinformatics Analysis Tool of Molecular Mechanism of Traditional Chinese Medicine; PPI, protein-protein interaction.

Chondrex, Inc.), tissue fixative solution (Beijing Jiuzhou Berlin Biotechnology Co., Ltd.), EDTA (cat. no. E8030; Beijing Solarbio Science & Technology Co., Ltd.), rat IL-6 ELISA kit (cat. no. CRE0005; Beijing 4A Biotech Co., Ltd.), rat IL-1β ELISA kit (cat. no. CRE0006; Beijing 4A Biotech Co., Ltd.), rat IL-17A ELISA kit (cat. no. CRE0021; Beijing 4A Biotech Co., Ltd.) and rat TNF-α ELISA kit (cat. no. CRE0003; Beijing 4A Biotech Co., Ltd.) were purchased.

Experimental drugs. JWGZSYZMD-related medicinal materials were purchased from the Pharmacy of Beijing University of Chinese Medicine and manufactured by Beijing Temages Pharmaceutical Co., Ltd.. This decoction comprises 10 g 'Gui Zhi' (*Ramulus Cinnamomi*; Guangdong*)*, 9 g 'Gan Cao' (Zhi; *Radix Glycyrrhizae Uralensis*; Inner Mongolia), 12 g 'Ma Huang' (*Herba Ephedrae*; Inner Mongolia), 12 g 'Bai Zhu' (*Rhizoma Atractylodis Macrocephalae*; Zhejiang), 9 g 'Bai Shao' (*Raidix Paeoniae Alba*; Anhui), 12 g 'Zhi Mu' (*Rhizoma Anemarrhenae*; Inner Mongolia), 12 g 'Sheng Jiang' (*Rhizoma Zingiberis Recens*; Sichuan), 12 g 'Fang Feng' (*Radix Saposhnikoviae*; Jilin), 12 g 'Bu Gu Zhi' (*Fructus Psoraleae*; Henan), 10 g 'Fu Zi' (*Radix Aconiti Lateralis Preparata*; Sichuan), 12 g 'Sang Zhi' (*Ramulus Mori*; Hebei) and 15 g 'Gu Sui Bu' (*Rhizoma Drynariae*; Guangdong). Each sample stock contained a total of 137 g crude drug preparation. In total, 2.283 g/kg crude drug is recommended, with the assumption that the average human body weight is 60 kg. The conversion factor of body surface area between humans and rats is 6.3 (22). Therefore, the dose to be administered to the rats was calculated to be 14.385 g/kg crude drug preparation, which equated to that administered to the medium dose group of animals. The high dose was double that of the

medium dose (28.770 g/kg) whereas the low dose was 50% of the medium dose (7.193 g/kg). The JWGZSYZMD was soaked in 10 volumes of water for 1 h, before being decocted for 1 h with 100˚C distilled water followed by filtration using a gauze. The aforementioned decoction step was repeated twice. The resulting preparation was diluted with distilled water to 0.7193, 1.4385 and 2.877 g/ml of crude drug for the low-, medium- and high-dose groups, respectively.

The clinical dosage of tripterygium glycoside for humans is 1.5 mg/kg (23) and the dose administered to rats was calculated to be 9.45 mg/kg. Tripterygium glycoside tablets (Zhejiang DND Pharmaceutical Co., Ltd.) were ground and diluted with distilled water to form a 0.945 mg/ml solution. Following preparation, the drug was stored in a refrigerator at 4˚C for future use. This solution was mixed well before use.

Experimental animals. The present study was assessed and approved by the Sub-Committee of Experimental Animal Ethics of Academic Committee of Beijing University of Traditional Chinese Medicine (approval no. BUCM-4-202109 0605-3104; Beijing, China).

A total of 60 SPF male Sprague Dawley rats (age, 6 weeks; weight, 180-200 g) were purchased from Spefford (Beijing) Biotechnology Co., Ltd. license number, SYXK (Jing) 2020-0033). The experimental animals were housed in the animal room of China-Japan Friendship Hospital (temperature, 23±2˚C; humidity, 65±5%; light, 12 h/day) with free access to clean drinking water and food during rearing. Animal health and behavior were monitored on a daily basis. A pathophysiological drop in body temperature was used as a humane endpoint and no rats had to be euthanized before the end of the experiment. Within 2 h of removal of ankle tissue, the rats

were euthanized by CO_2 inhalation at 30% vol/min. Death was confirmed by the lack of breathing, stiffness and dilated pupils in the rats, after which the CO_2 inhalation ceased and the rats were observed for 2 min to verify death. After euthanasia, the animals were stored in a designated freezer at ~-20˚C.

Establishment of CIA model. A total of 6 rats were randomly assigned into the control group, whereas the other 54 rats were used to establish the CIA model by injecting bovine collagen II/Freund's incomplete adjuvant at the tail root (n=6/group). A bovine collagen II solution of 4 g/l was prepared with 0.1 mol/l glacial acetic acid (Xilong Science Co., Ltd.) and was added dropwise to the syringe. An equal volume of collagen II acetate solution was mixed with incomplete Freund's adjuvant in an ice bath until fully emulsified. Use a blender(IKA) to homogenize was performed for 3 min and halted for 30 sec at each cycle, with 10 cycles performed in total until the emulsion dripped into the water without diffusion. The homogenized collagen was then wrapped in tinfoil and placed on ice ready for injection. The skin at the base of the rat's tail was wiped using a cotton ball with alcohol, before 200 μl of the collagen mixture was injected subcutaneously at the right side of the base of the rat's tail. After 1 week, 100 μl of the collagen mixture was injected at the left side of the base of the tail (24).

Drug-dosing interventions. Rats were assessed 1 week after the second injection using a joint score from 0-4 as follows: i) 0, normal or no inflammation of the paws; ii) 1, swelling or slight redness of the toe joints; iii) 2, redness and swelling of the toe joints and paws; iv) 3, redness and swelling of the entire paw below the ankle joint; and v) 4, severe redness and swelling of the ankle joint with signs of joint deformation. Rats with a total score of >4 on both sides were selected for further study, resulting in 30 rats being randomly selected and divided into the CIA model, JWGZSYZMD low-dose, JWGZSYZMD medium-dose, JWGZSYZMD high-dose and tripterygium glycoside groups. Saline was administered to the CIA model group, whereas the other groups were given the corresponding drug at a dose of 1 ml/100 g body weight for 21 consecutive days.

Histopathological analysis. After 21 consecutive days of treatment, rats were anesthetized by an intraperitoneal injection of 30 mg/kg pentobarbital before the left ankle joint was removed from the excess tissue and muscle. The joint tissues were 0.3 cm thick and fixed with 10% formalin for 72 h at 25˚C, before being added to 10% EDTA for decalcification. The 10% EDTA solution was changed once a week for 8 consecutive weeks until the completion of decalcification. After dehydration, paraffin embedding, section to 5 μm and hematoxylin in 5 min and eosin in 1 min (H&E) staining were performed in 35˚C and rat joint pathology was observed using a light microscope.

Detection of synovial inflammatory factors in rats by ELISA. The right ankle joint of the rat was dissected from the medial side and the skin was dissected to open the ankle joint cavity to obtain the synovial tissue. The synovium was separated using ophthalmic scissors under a dissecting microscope and saline was added for adequate grinding. The grinding solution was centrifuged at 1,006.2 x g) for 10 min with 20˚C before the supernatant was collected and stored at -80˚C for future use. The expression levels of IL-1β, IL-6, IL-17A and TNF-α

in each group were detected using ELISA kits according to the manufacturer's protocols.

Reverse transcription-quantitative PCR. TRIzol® solution (Invitrogen; Thermo Fisher Scientific, Inc.) was used to extract the total RNA from the synovial membrane of the ankle joint tissue. Reverse transcription was performed using the All-in-One™ First-Strand cDNA Synthesis Kit (cat. no. AORT-0050; GeneCopoeia, Inc.) in accordance with the manufacturer's instructions. after qPCR in the ABI7500 system (Thermo Fisher Scientific, Inc.). qPCR was performed using the Platinum® SYBR® Green Realtime PCR Master Mix (cat. no. QPK-201; Toyobo Life Science) as follows: Initial denaturation at 95˚C for 30 sec, followed by 40 cycles of 95˚C for 10 sec, the annealing and extension temperatures are maintained at 60˚C for 30 sec. The $2^{-\Delta\Delta Cq}$ method (25) was used to quantify mRNA expression. Primer sequences are listed in Table V.

Statistical analysis. SPSS (version 26.0; IBM Corp.) and GraphPad prism (version 8.0; Dotmatics) were used for statistical analysis. Data normality was analyzed using the Shapiro-Wilk test. Protein expression levels of IL-1β and TNF-α and mRNA expression levels of IL-6, IL-1β and IL-17A are presented the mean ± standard deviation. The joint scores of rats, protein expression of IL-17A and IL-6 and mRNA expression levels of TNF-α were presented as the median (interquartile range). Paired data of joint scores were analyzed using Wilcoxon's signed-rank test followed by Bonferroni correction. One-way ANOVA followed by Tukey's test was used for statistical analysis of parametric data, whereas the Kruskal-Wallis H test followed by Dunn's test for statistical analysis of non-parametric data (Protein expression of IL-17A and IL-6, mRNA expression of TNF-α) for two-group comparisons and two-group comparisons for joint scores of rats (after treatment) subsequently followed by Bonferroni correction. P<0.05 was considered to indicate a statistically significant difference.

Results

Drugs and disease corresponding targets. Through TCMSP and BATMAN-TCM database screening, searches of 'Gui Zhi' (*Ramulus Cinnamomi*), 'Bai Zhu' (*Rhizoma Atractylodis Macrocephalae*), Gan Cao (Zhi; *Radix Glycyrrhizae Uralensis*), 'Ma Huang' (*Herba Ephedrae*), 'Bai Shao' (*Raidix Paeoniae Alba*), 'Zhi Mu' (*Rhizoma Anemarrhenae*), 'Sheng Jiang' (*Rhizoma Zingiberis Recens*), 'Fang Feng' (*Radix Saposhnikoviae*), 'Bu Gu Zhi' (*Fructus Psoraleae*), 'Fu Zi' (*Radix Aconiti Lateralis Preparata*), 'Sang Zhi' (*Ramulus Mori*) and 'Gu Sui Bu' (*Rhizoma Drynariae*) yielded a total of 69 potentially effective active ingredients contained within JWGZSYZMD. In addition, 4,792 RA-related gene targets were obtained through the Genecards database, including 191 targets possibly affected by JWGZSYZMD.

Drug-active component-disease target regulatory networks. Cytoscape 3.7.2 software was used to construct the 'drug-active ingredient-disease target' network of JWGZSYZMD in the regulation of RA (Fig. 2). The number of node connections in the network was calculated and the top 30 active ingredients
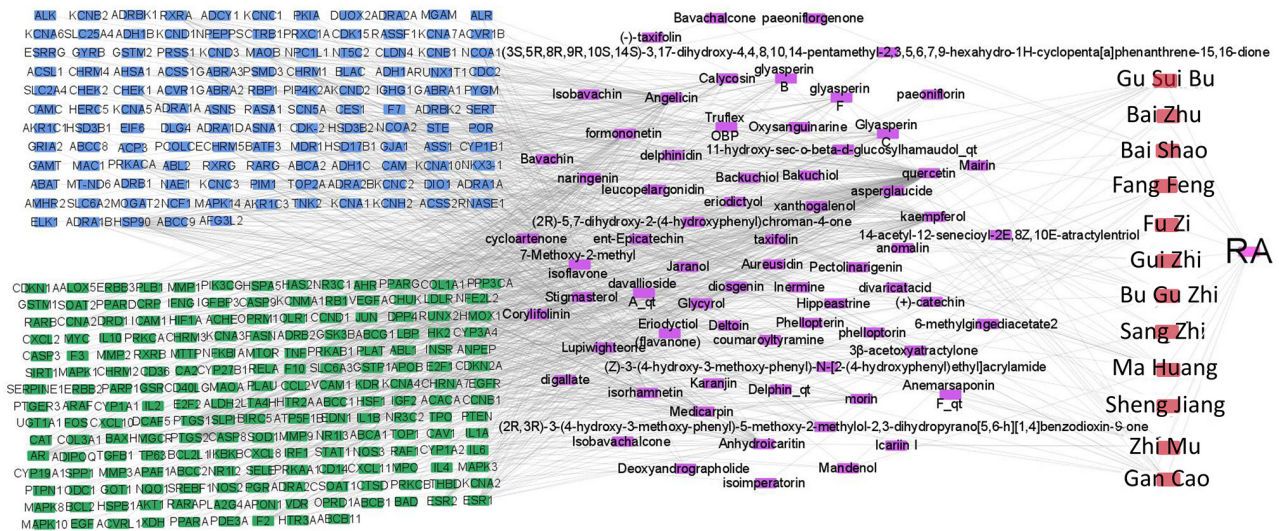
Figure 2. Drug-active component-disease-target regulatory networks. The red nodes indicate the composition of JWGZSYZMD for the treatment of RA, the purple nodes indicate the active ingredients of Traditional Chinese Medicine present in each drug composition, the blue and green nodes indicate the targets corresponding to each active ingredient and the targets of JWGZSYZMD for the regulation of RA are marked as green. RA, rheumatoid arthritis; JWGZSYZMD, Jiawei Guizhishaoyaozhimu Decoction.

with the highest number of targets were selected to be potential active ingredients for RA treatment. These were quercetin, angelicin, kaempferol, 7-methoxy-2-methyl isoflavone, naringin, formononetin, isorhamnetin, icaritin dehydrated, alfalfa toxin, stigmasterol, glyasperin C, calycosin, glyasperin B, lupiwighteone, glyasperin F, Inermine, morin, aureusidin, diosgenin, catechin, jaranol, taxifolin, xanthogalenol, pectolinarigenin, phellopterin, glycyrol, hippeastrine, deltoin, coumaroyltyramine and eriodictyol (Table I).

PPI predictions of core targets of JWGZSYZMD during therapy of RA. The STRING database and Cytoscape were used to analyze and visualize the targets of RA regulation by JWGZSYZMD. The STRING database used PPI network (Fig. 3A). The top 30 targets were found to mainly involve factors associated with inflammation (TNF, IL-6, IL-1B, prostaglandin-endoperoxide synthase, IL-10 and IL-8), key node proteins of inflammatory pathways (AKT1, JUN, MAPK3, nitric oxide synthase 3 and MMP9), synovial angiogenesis processes [VEGFA and hypoxia-inducible factor (HIF) 1A], apoptosis and cycle regulation (caspase 3, Myc, cyclin D1, PTEN and Fos), hormone regulation (EGFR, peroxisome proliferator-activated receptor γ, estrogen receptor 1 and EGF) and chemokines (chemokine ligand 2) (Fig. 3B).

KEGG predictions of key pathways of JWGZSYZMD during RA therapy. The pathways affected by JWGZSYZMD treatment of RA mainly involved inflammation-related pathways (such as 'IL-17 signaling pathway', 'TNF signaling pathway', 'PI3K/Akt signaling pathway', 'MAPK signaling pathway', 'NF-κB signaling pathway', 'Toll-like receptor signaling pathway' and 'NOD-like receptor signaling pathway'), T cell differentiation-related signaling ('Th17 cell differentiation', 'T cell receptor signaling pathway' and 'Th1 and Th2 cell differentiation'), neovascularization signaling ('HIF-1 signaling pathway' and 'VEGF signaling pathway'), 'Osteoclast differentiation signaling' and 'Apoptosis' (Fig. 4).

Molecular docking verification. The AutoDock Vina program was used to perform molecular docking of the top 30 active ingredients onto IL-1β, IL-6, IL-17A and TNF-α in the 'drug-active ingredient-disease target' network, where the lowest binding energy was calculated. The lower the binding energy, the stronger the binding force between the chemical composition and the target. It is generally considered that the binding energy of <-5.0 kJ/mol suggests good binding activity, whilst <-7.0 kJ/mol would suggest strong binding activity (26). In the present study, the minimum binding energy for molecular docking between active components and target sites was ≤-5.0 kJ/mol, whereas 76 molecules demonstrated docking binding energy of ≤-7.0 kJ/mol (Table II). This finding suggested that the binding ability between the potential active components and target sites is viable. The three results with the strongest binding activity found were IL-17 with diosgenin, TNF with eriodictyol and IL-17 with glycyrol, which were then visualized using the Pymol and Ligplot software (Fig. 5) (27).

Effect of JWGZSYZMD on joint score of rats. The joint score of rats in the five treatment groups was measured and was defined as the baseline. No statistically significant differences were found between groups (Table III). After 21 days of the drug treatments, the joint scores of JWGZSYZMD high-dose and the tripterygium glycoside groups significantly decreased joint score compared with that in the CIA model group (P<0.05). By contrast, rats in the control group exhibited a joint score of 0 throughout the experiment. There no statistically significant difference in the joint scores of rats treated with low-, medium- or high-dose JWGZSYZMD.

Effect of JWGZSYZMD on pathology in rats. The staining results demonstrated that the joint cavity structure of rats in the control group was normal, as no infiltration of monocytes or bone erosion was observed in the synovium. However, a large number of inflammatory cells were be observed in the synovium of rats in the CIA model group, where cartilage

Table I. Top 30 potential active components of Jiawei Guizhishaoyaozhimu Decoction for the treatment of rheumatoid arthritis.

Compound names	ID	Active ingredient	Oral bioavailability	Drug likeness	Number of targets
Ma Huang (*Herba Ephedrae*)	MOL000098	Quercetin	46.43	0.28	152
Bu Gu Zhi (*Fructus Psoraleae*) [a]	NA	Angelicin	NA	NA	74
Sang Zhi (*Ramulus Mori*), Ma Huang (*Herba Ephedrae*), Bai Shao (*Raidix Paeoniae Alba*), Gu Sui Bu (*Rhizoma Drynariae*), Zhi Mu (*Rhizoma Anemarrhenae*) and Gan Cao (Zhi; *Radix Glycyrrhizae Uralensis*)	MOL000422	Kaempferol	41.88	0.24	68
Gan Cao (Zhi; *Radix Glycyrrhizae Uralensis*)	MOL003896	7-Methoxy-2-methyl isoflavone	42.56	0.20	44
Gu Sui Bu (*Rhizoma Drynariae*), Ma Huang (*Herba Ephedrae*) and Gan Cao (Zhi; *Radix Glycyrrhizae Uralensis*)	MOL004328	Naringenin	59.29	0.21	40
Gan Cao (Zhi; *Radix Glycyrrhizae Uralensis*)	MOL000392	Formononetin	69.67	0.21	39
Gan Cao (Zhi; *Radix Glycyrrhizae Uralensis*)	MOL000354	Isorhamnetin	49.60	0.31	38
Zhi Mu (*Rhizoma Anemarrhenae*)	MOL004373	Anhydroicaritin	45.41	0.44	38
Gan Cao (Zhi; *Radix Glycyrrhizae Uralensis*)	MOL002565	Medicarpin	49.22	0.34	35
Sheng Jiang (*Rhizoma Zingiberis Recens*), Ma Huang (*Herba Ephedrae*) and Gu Sui Bu (*Rhizoma Drynariae*)	MOL000449	Stigmasterol	43.83	0.76	35
Gan Cao (Zhi; *Radix Glycyrrhizae Uralensis*)	MOL004811	Glyasperin C	45.56	0.40	25
Gan Cao (Zhi; *Radix Glycyrrhizae Uralensis*)	MOL000417	Calycosin	47.75	0.24	23
Gan Cao (Zhi; *Radix Glycyrrhizae Uralensis*)	MOL004808	Glyasperin B	65.22	0.44	22
Gan Cao (Zhi; *Radix Glycyrrhizae Uralensis*)	MOL003656	Lupiwighteone	51.64	0.37	22
Gan Cao (Zhi; *Radix Glycyrrhizae Uralensis*)	MOL004810	Glyasperin F	75.84	0.54	19
Gan Cao (Zhi; *Radix Glycyrrhizae Uralensis*)	MOL001484	Inermine	75.18	0.54	18
Sang Zhi (*Ramulus Mori*)	MOL000737	Morin	46.23	0.27	18
Gu Sui Bu (*Rhizoma Drynariae*)	MOL001978	Aureusidin	53.42	0.24	18
Zhi Mu (*Rhizoma Anemarrhenae*)	MOL000546	Diosgenin	80.88	0.81	17
Gu Sui Bu (*Rhizoma Drynariae*), Bai Shao (*Raidix Paeoniae Alba*), Ma Huang (*Herba Ephedrae*) and Gui Zhi (*Ramulus Cinnamomi*)	MOL000492	Catechin	54.83	0.24	15
Gan Cao (Zhi; *Radix Glycyrrhizae Uralensis*)	MOL000239	Jaranol	50.83	0.29	14
Gui Zhi (*Ramulus Cinnamomi*) and Ma Huang (*Herba Ephedrae*)	MOL004576	Taxifolin	57.84	0.27	14
Gu Sui Bu (*Rhizoma Drynariae*)	MOL009091	Xanthogalenol	41.08	0.32	14
Ma Huang (*Herba Ephedrae*)	MOL005842	Pectolinarigenin	41.17	0.30	13
Fang Feng (*Radix Saposhnikoviae*)	MOL002644	Phellopterin	40.19	0.28	13
Gan Cao (Zhi; *Radix Glycyrrhizae Uralensis*)	MOL002311	Glycyrol	90.78	0.67	12
Zhi Mu (*Rhizoma Anemarrhenae*)	MOL004497	Hippeastrine	51.65	0.62	12
Fu Zi (*Rhizoma Typhonii Gigantei*)	MOL002392	Deltoin	46.69	0.37	12
Zhi Mu (*Rhizoma Anemarrhenae*)	MOL000631	Coumaroyltyramine	112.90	0.20	11
Gu Sui Bu (Rhizoma Drynariae) and Ma Huang (Herba Ephedrae)	MOL005190	Eriodictyol	71.79	0.24	11

[a]'Bu Gu Zhi' (*Fructus Psoraleae*) was not included in the Traditional Chinese Medicine Systems Pharmacology Database; therefore, it was analyzed using the Bioinformatics Analysis Tool of Molecular Mechanism of Traditional Chinese Medicine. After screening with a score cut-off ≥20 and P<0.05, the chemical composition of this compound met the screening conditions (10). NA, not applicable.

erosion could also be seen. By contrast, synovial inflammatory cell infiltration and cartilage erosion were markedly milder in the low-dose and medium-dose groups of JWGZSYZMD compared with those in the CIA model group. Only a small
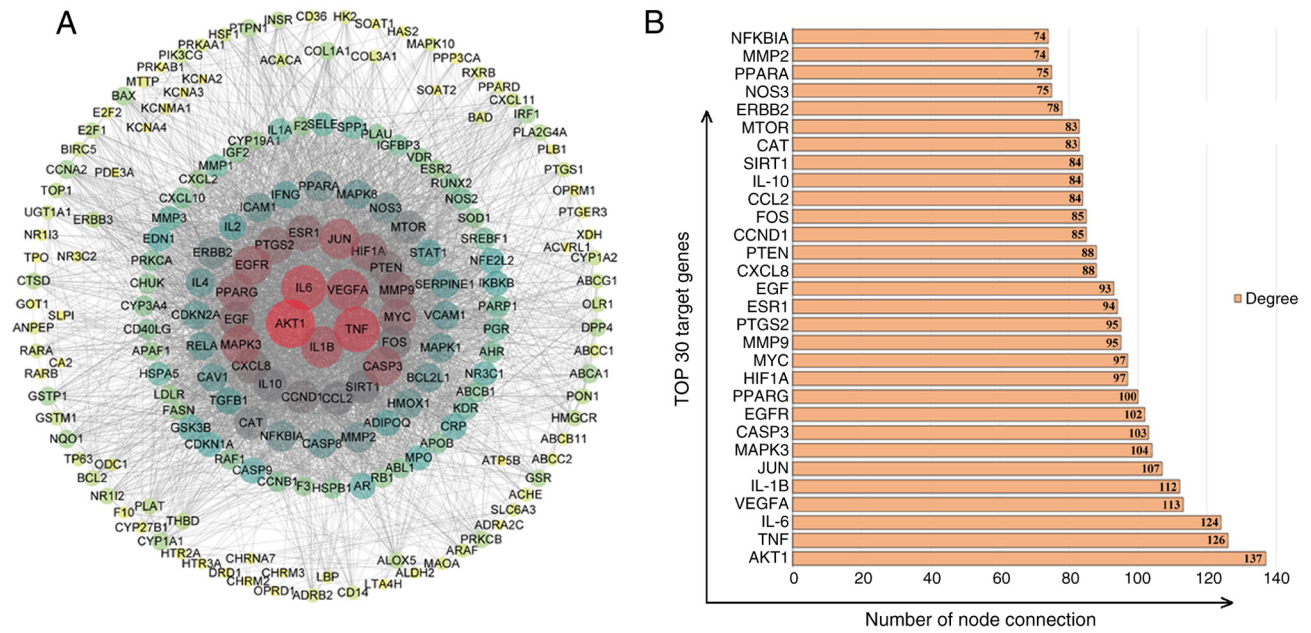
Figure 3. Protein-protein interaction prediction of core targets of JWGZSYZMD during therapy of RA. (A) The protein-protein interaction network of JWGZSYZMD and RA intersection targets, where size and color of nodes were related to the core degree of nodes in the network. Targets at the core of the network are marked in red. (B) Targets in the top 30, ranked in terms of the number of node connection in the descending order. RA, rheumatoid arthritis; JWGZSYZMD, Jiawei Guizhishaoyaozhimu Decoction.
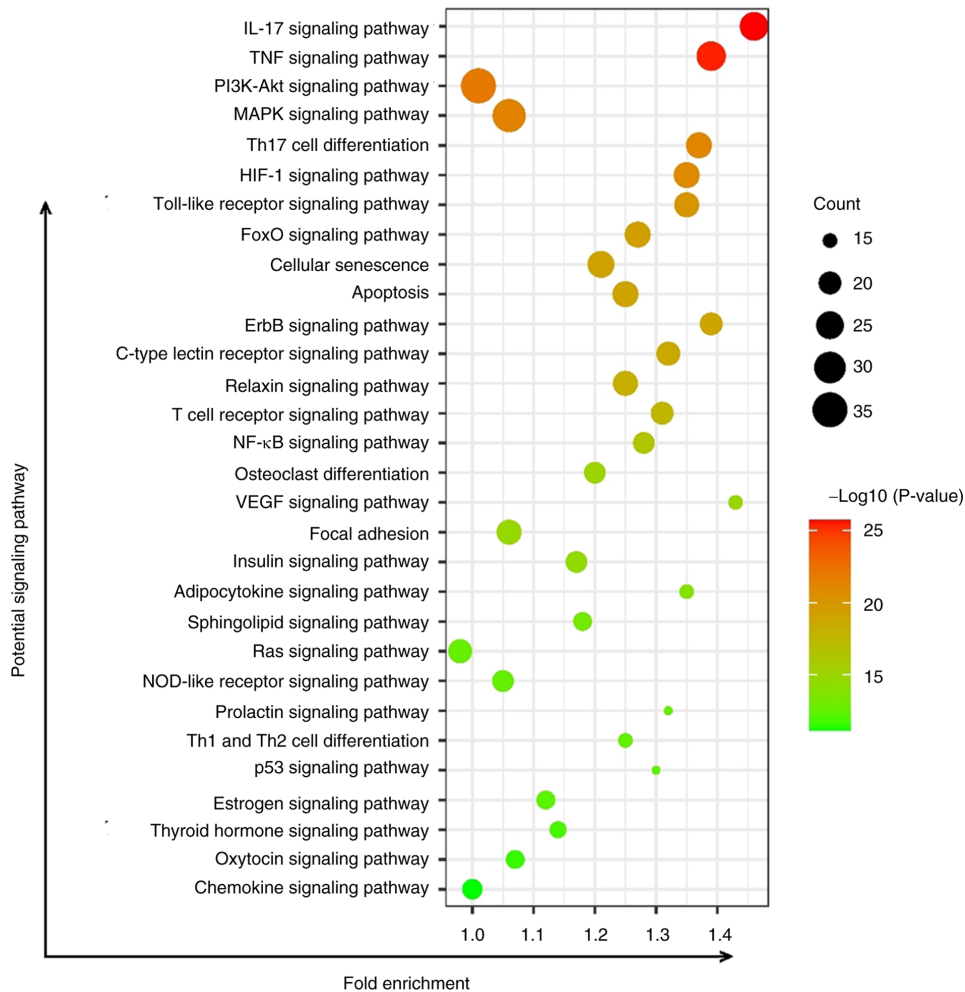

Figure 4. KEGG pathway enrichment analysis. The bubble size represented the number of targets coincident with this path in the regulation of rheumatoid arthritis by Jiawei Guizhishaoyaozhimu Decoction and the color represented the P-value of KEGG enrichment. KEGG, Kyoto Encyclopedia of Genes and Genomes.

Table II. Molecular docking results of the active ingredients of Jiawei Guizhishaoyaozhimu Decoction to inflammatory cytokines.

Active ingredient	Binding energy to IL-1β (kcal/mol)	Binding energy to IL-6, kcal/mol)	Binding energy to IL-17 (kcal/mol)	Binding energy to TNF-α (kcal/mol)
Quercetin	-7.3	-6.8	-7.9	-8.8
Angelicin	-5.8	-6.1	-6.7	-7.2
Kaempferol	-7.2	-6.7	-7.6	-8.6
7-Methoxy-2-methyl isoflavone	-6.2	-6.2	-8.0	-8.3
Naringenin	-7.3	-6.9	-8.2	-8.3
Formononetin	-6.5	-6.8	-7.7	-8.4
Isorhamnetin	-7.0	-7.0	-7.8	-8.0
Anhydroicaritin	-6.9	-7.1	-8.3	-6.6
Medicarpin	-6.8	-6.5	-7.4	-8.3
Stigmasterol	-7.2	-6.6	-8.3	-6.5
Glyasperin C	-7.0	-6.7	-7.9	-5.8
Calycosin	-6.6	-6.6	-8.0	-6.5
Glyasperin B	-6.5	-6.5	-8.6	-5.9
Lupiwighteone	-7.1	-6.8	-7.9	-6.6
Glyasperin F	-7.5	-7.1	-8.7	-6.7
Inermine	-7.1	-7.0	-8.3	-7.0
Morin	-7.2	-6.7	-7.7	-8.6
Aureusidin	-7.3	-7.2	-8.4	-8.5
Diosgenin	-8.0	-7.5	-10.3	-7.4
Catechin	-6.6	-7.2	-7.4	-6.9
Jaranol	-6.2	-6.5	-7.7	-7.6
Taxifolin	-7.0	-7.3	-7.6	-7.6
Xanthogalenol	-6.5	-6.1	-7.7	-6.0
Pectolinarigenin	-6.6	-6.8	-7.6	-7.7
Phellopterin	-5.8	-6.6	-7.4	-8.1
Glycyrol	-7.2	-6.8	-8.9	-6.7
Hippeastrine	-7.0	-7.4	-8.4	-8.3
Deltoin	-7.4	-6.0	-7.5	-7.3
Coumaroyltyramine	-5.8	-6.3	-8.0	-7.9
Eriodictyol	-7.0	-7.3	-7.9	-9.0

amount of inflammatory cell infiltration was observed in the high-dose group of JWGZSYZMD and the tripterygium glycoside group (Fig. 6).

Effects of JWGZSYZMD on the mRNA expression levels of synovial inflammatory factors in rats. The mRNA expression levels of the inflammatory factors IL-6, TNF-α, IL-1β and IL-17A in the CIA model rats were significantly increased compared with those in the control group (P<0.05; Fig. 7). The expression levels of IL-6 and TNF-α in the tripterygium glycoside group were significantly increased compared with those in the control group (P<0.05). The expression levels of IL-1β, TNF-α and IL-6 in the low-, medium- and high-dose JWGZSYZMD groups and IL-17A in the low- and medium-dose JWGZSYZMD groups were significantly increased compared with those in the control group (P<0.05). The expression levels of TNF-α mRNA in the low-, medium- and high-dose JWGZSYZMD groups were significantly lower compared with that in the CIA model group (P<0.05). The expression levels of IL-1β in the low-, medium- and high-dose

JWGZSYZMD groups and IL-6 and IL-17A in the medium- and high-dose JWGZSYZMD groups were significantly lower compared with that in the CIA model group (P<0.05). The expression levels of IL-1β, IL-6 and IL-17A in the high-dose JWGZSYZMD group were significantly lower compared with that in the low-dose JWGZSYZMD group (P<0.05). The expression levels of IL-1β and IL-6 in the high-dose JWGZSYZMD group were decreased compared with that in the medium-dose JWGZSYZMD group (P<0.05). A dose-dependent effect was observed with increasing concentrations of JWGZSYZMD treatment. The expression levels of IL-6, TNF-α, IL-1β and IL-17A in the tripterygium glycoside group was significantly decreased compared with that in the CIA model group (P<0.05). The expression levels of IL-1β, IL-6, IL-17A and TNF-α in the tripterygium glycoside group were significantly lower compared with that in the low-dose JWGZSYZMD group (P<0.05). The expression levels of IL-1β, IL-6 and TNF-α in the tripterygium glycoside group were decreased compared with that in the medium-dose JWGZSYZMD group (P<0.05).
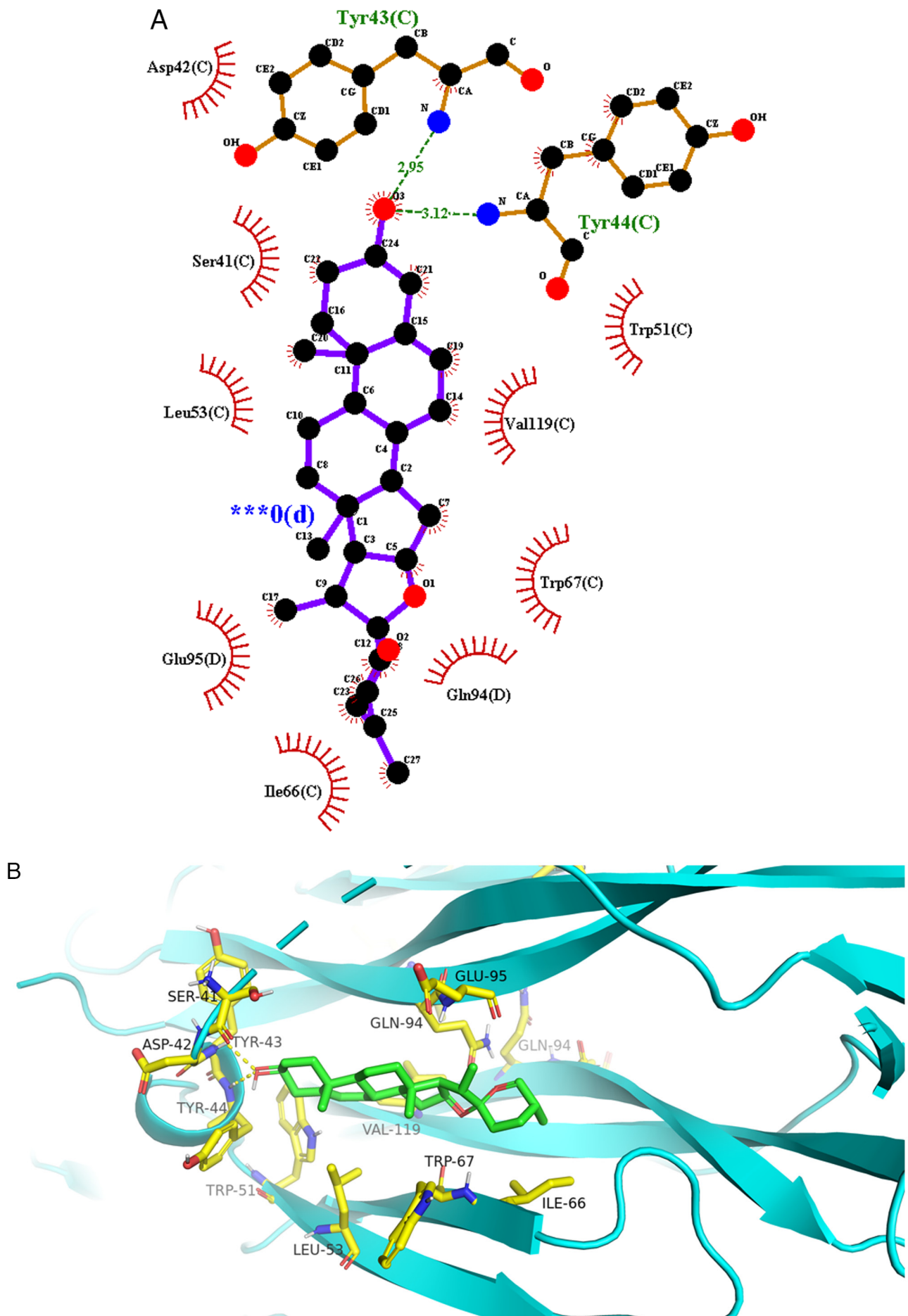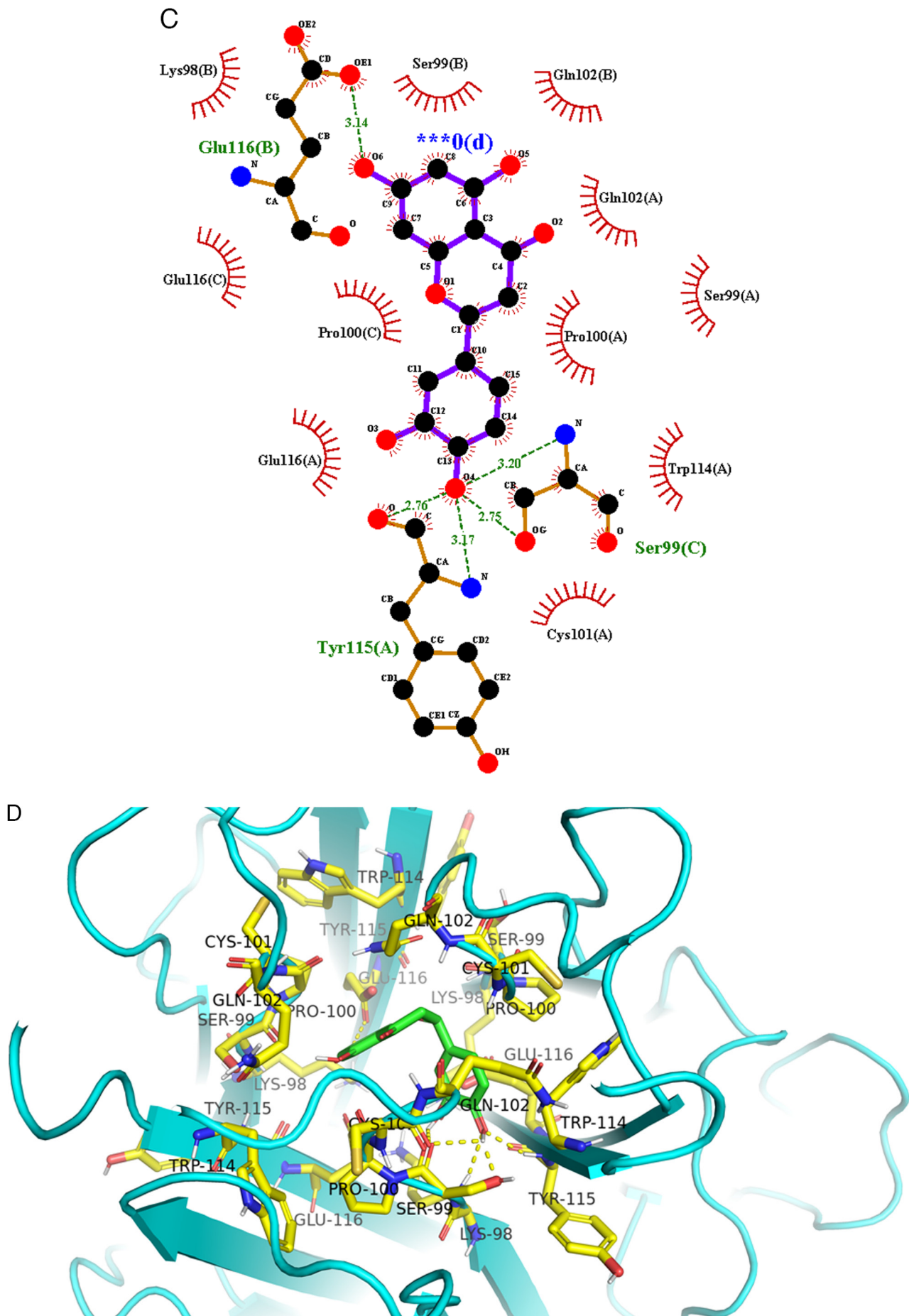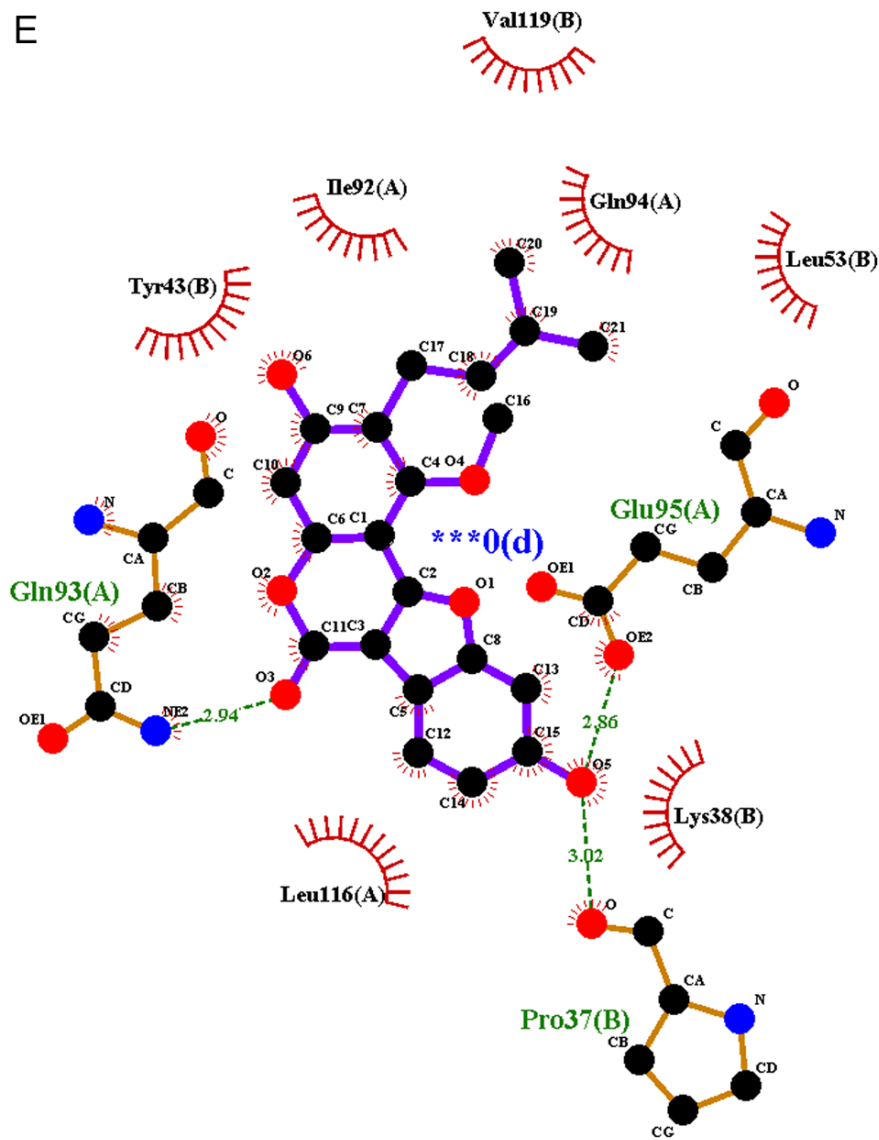
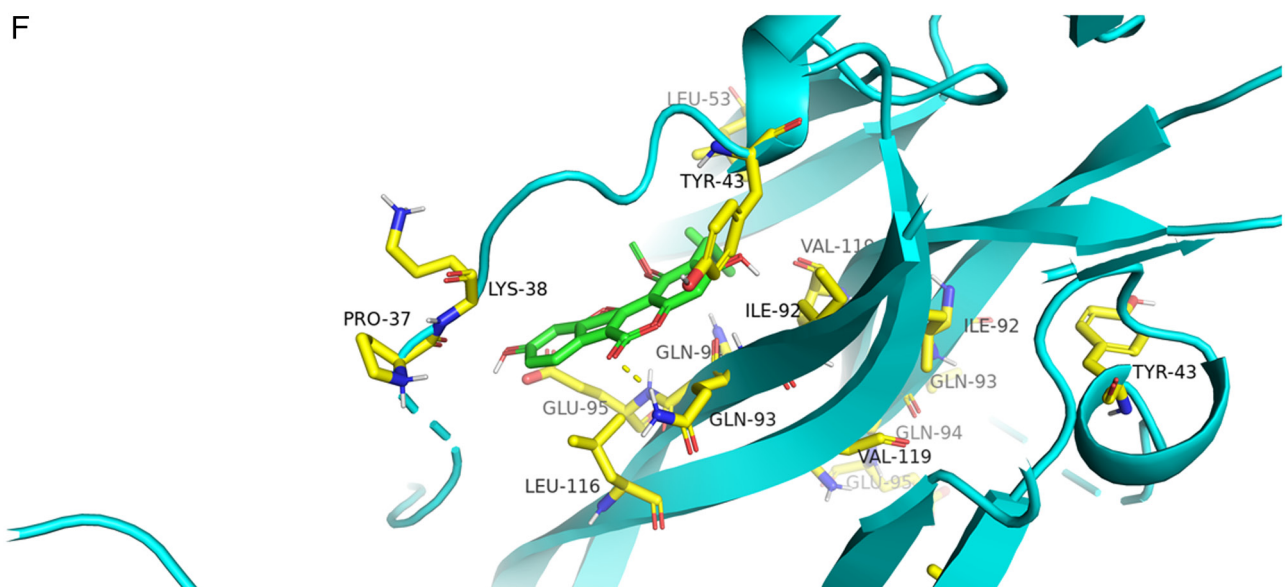Figure 5. Continued.

Figure 5. Continued.

Figure 5. Molecular docking verification. Specifically, 'IL-17-diosgenin', 'TNF-eriodictyol' and 'IL-17-glycyrol' are the three molecules with the strongest binding activity and the docking results were visualized. (A) 2D results of the docking of IL-17 with diosgenin. (B) The figure shows the 3D results of the docking of IL-17 with diosgenin. (C) The figure shows the 2D results of the docking of TNF with eriodictyol. (D) The figure shows the 3D results of the docking of TNF with eriodictyol. (E) The figure shows the 2D results of the docking of IL-17 with glycyrol. (F) The figure shows the 3D results of the docking of IL-17 with glycyrol.

Table III. Joint scores of CIA rats before and after treatment with JWGZSYZMD.

Treatment group	Joint score before treatment	Joint score after treatment	Z-score	P-value
Control	0.00 (0.00, 0.00)	0.00 (0.00, 0.00)	0.000	1.000
CIA model	6.50 (6.00, 8.00)	7.50 (6.75, 8.00)	-1.134	>0.999
JWGZSYZMD low-dose	7.00 (5.00, 8.00)	6.00 (5.00, 7.00)	-1.633	0.612
JWGZSYZMD medium-dose	7.00 (6.00, 7.25)	5.50 (5.00, 6.25)	-1.633	0.612
JWGZSYZMD high-dose	6.00 (5.75, 7.25)	5.00 (5.00, 6.00)[a]	-1.604	0.654
Tripterygium glycoside	7.00 (5.75, 8.00)	5.00 (4.00, 6.00)[a]	-1.841	0.396
H	1.100	14.179		
P-value	0.894	0.007		

Joint scores of rats (before vs. after treatment) were analyzed using Wilcoxon's signed-rank test followed by Bonferroni correction. Joint scores of rats (after treatment) were analyzed using the Kruskal-Wallis H test followed by Dunn's test and subsequently followed by Bonferroni correction for each comparison. Data were presented as the median (quartile 1, quartile 3). [a]$P<0.05$ vs. CIA model group. JWGZSYZMD, Jiawei Guizhishaoyaozhimu Decoction; CIA, collagen II-induced arthritis.
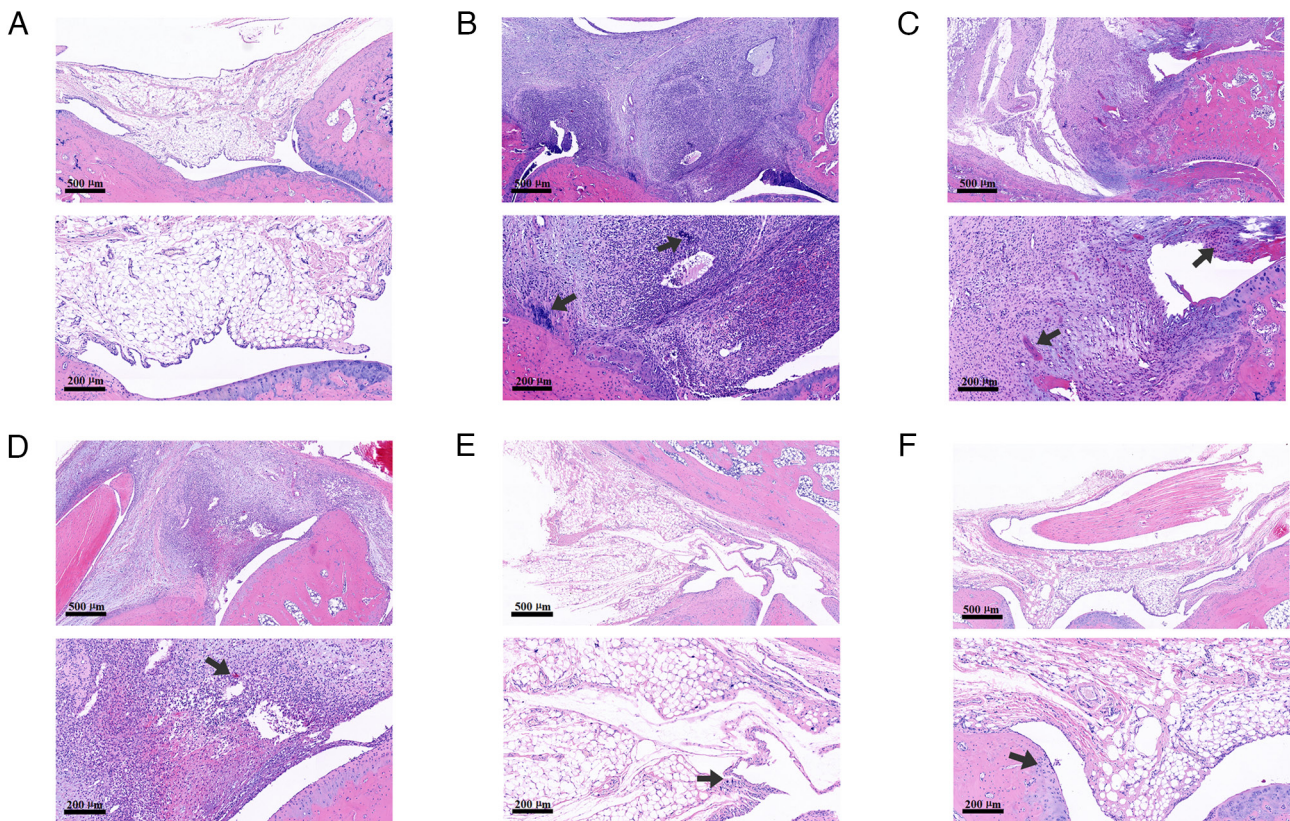

Figure 6. Effect of JWGZSYZMD on the joint pathology of rats with CIA. (A) Control group, (B) CIA model group, (C) JWGZSYZMD low-dose group. (D) JWGZSYZMD medium-dose group. (E) JWGZSYZMD high-dose group and (F) tripterygium glycoside group. CIA, collage II-induced arthritis; JWGZSYZMD, Jiawei Guizhishaoyaozhimu Decoction. Black arrow: Inflammatory cells, Blue or red colouring of the nucleus.

Effects of JWGZSYZMD on the protein expression levels of synovial inflammatory factors in rats. The protein expression levels of synovial inflammatory factors IL-6, TNF-α, IL-1β and IL-17A were analyzed by ELISA. The results suggested that the protein expression levels of these factors in the CIA model rats, all JWGZSYZMD treatment groups and the tripterygium glycoside group were significantly compared with those in the control group (P<0.01; Table IV). The protein expression levels of IL-1β and IL-6 in the high-dose JWGZSYZMD group and IL-17 protein expression levels in the medium-dose JWGZSYZMD group were significantly lower compared with those in the CIA model group (P<0.05). The protein expression levels of TNF-α in the medium- and high-dose JWGZSYZMD group and IL-17A protein expression levels in the high-dose JWGZSYZMD group were significantly lower compared with those in the CIA model group (P<0.01). The protein expression levels of IL-17A in the medium-dose JWGZSYZMD group and IL-6 in the
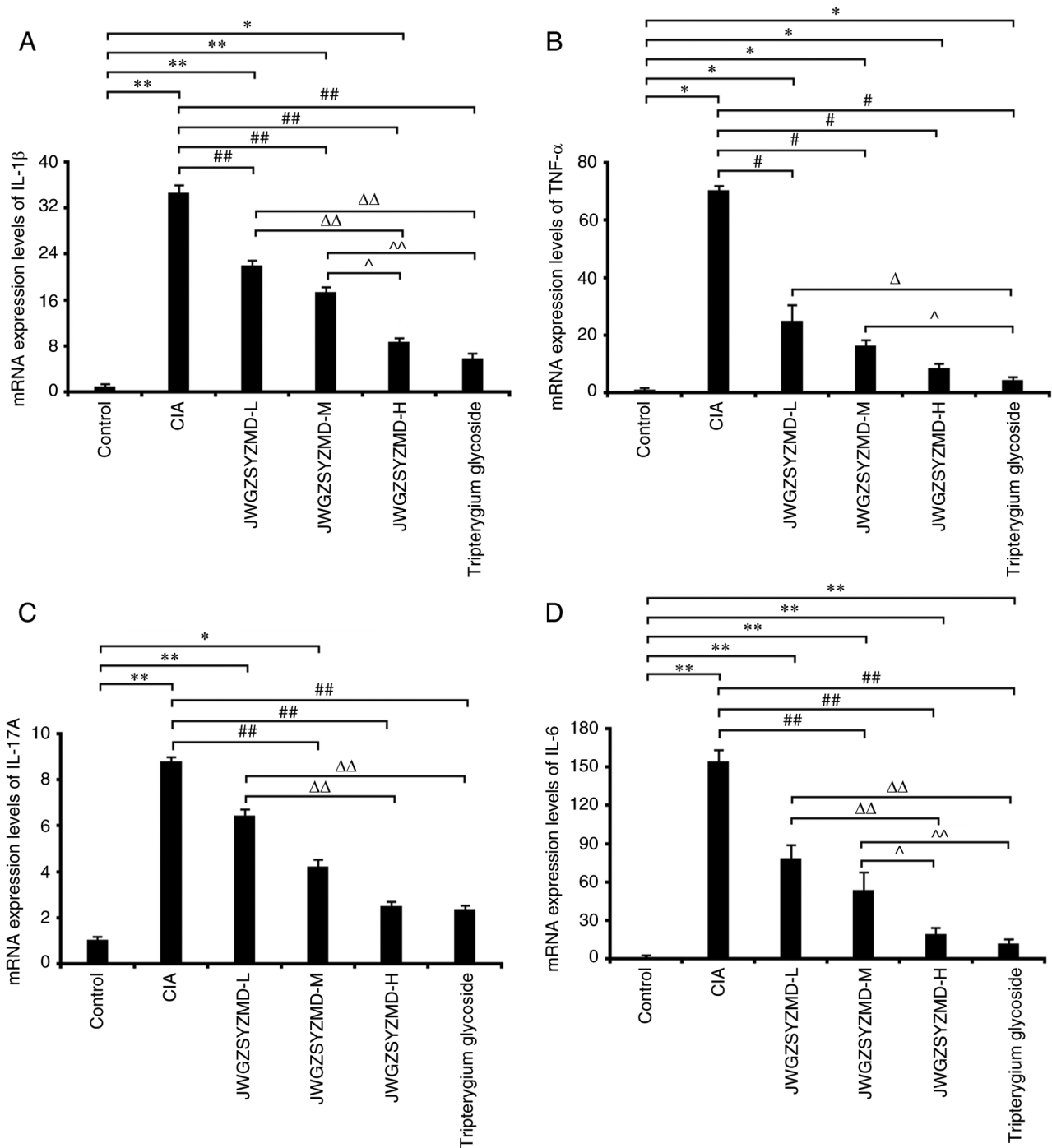
Figure 7. mRNA expression levels of synovial inflammatory factors in rats treated with JWGZSYZMD. Expression levels of (A) IL-6, (B) TNF-α, (C) IL-1β and (D) IL-17A in the synovium of rats in each treatment group. One-way ANOVA followed by Tukey's test was used to analyze the expression levels of IL-6, IL-1β and IL-17A, whereas the Kruskal-Wallis H test followed by Dunn's test was used to analyze the expression levels of TNF-α. *P<0.05, **P<0.01 vs. Control Group. #P<0.05, ##P<0.01 vs. CIA model Group. ^P<0.05, ^^P<0.01 vs. JWGZSYZMD-L. ^P<0.05, ^^P<0.01 vs. JWGZSYZMD-M. JWGZSYZMD, Jiawei Guizhishaoyaozhimu Decoction; L, low; M, medium; H, high; CIA, collagen II-induced arthritis.

high-dose JWGZSYZMD group were significantly lower compared with those in the low-dose JWGZSYZMD group (P<0.05). The protein expression levels of TNF-α and IL-17A protein expression in the high-dose JWGZSYZMD group were significantly lower compared with those in the low-dose JWGZSYZMD group (P<0.01). A dose-dependent effect of JWGZSYZMD on protein expression levels of the synovial inflammatory factors was observed. The protein expression levels of IL-6, TNF-α, IL-1β and IL-17A in the tripterygium glycoside group was significantly lower compared with those in the CIA model group (P<0.01). The protein expression levels of TNF-α, IL-6, IL-1β and IL-17 in the tripterygium glycoside group were significantly lower compared with those in the low-dose JWGZSYZMD group (P<0.05). The protein expression levels of IL-17, IL-6 and TNF-α in the tripterygium glycoside group were significantly lower compared with those in the medium-dose JWGZSYZMD group (P<0.05).

Table IV. Protein expression levels of synovitis inflammatory factors IL-6, TNF-α, IL-1β and IL-17A in CIA mice treated with JWGZSYZMD.

Treatment group	Inflammatory factor (pg/ml)			
	IL-1β, mean ± SD	TNF-α, mean ± SD	IL-17A, median (Q1, Q3)	IL-6, median (Q1, Q3)
Control	3.118±1.507	2.596±1.226	1.346 (0.782, 1.852)	2.332 (1.982, 6.891)
CIA model	78.560±24.079[a]	160.328±36.997[a]	31.827 (22.443, 36.443)[a]	466.148 (225.123, 594.994)[a]
JWGZSYZMD low-dose	60.644±11.951[a]	122.052±33.630[a]	23.722 (20.789, 28.861)[a]	350.171 (265.022, 383.308)[a]
JWGZSYZMD medium-dose	45.612±23.427[a]	82.914±18.868[a,bb]	16.872 (15.448, 21.348)[a,b,c]	239.062 (129.033, 300.533)[a]
JWGZSYZMD high-dose	34.719±12.894[a,b]	48.809±23.509[a,bb,cc]	15.732 (8.170, 16.700)[a,bb,cc]	166.018 (82.241, 240.509)[a,b,c]
Tripterygium glycoside	26.067±4.203[a,bb,c]	27.925±16.740[a,bb,cc,dd]	11.848 (5.066, 15.653)[a,bb,c,d]	90.638 (63.794, 131.868)[a,bb,cc,d]
F	55.916	52.278		
H			29.075	27.223
P-value	2.6653x10^{-14}	6.5479x10^{-14}	0.000022	0.000052

IL-1β and TNF-α protein expression levels were analyzed using one-way ANOVA followed by Tukey's test. IL-17A and IL-6 protein expression levels were analyzed using Kruskal-Wallis H test followed by Dunn's test. [a]$P<0.01$ vs. Control; [b]$P<0.05$, [bb]$P<0.01$ vs. CIA model; [c]$P<0.05$, [cc]$P<0.01$ vs. JWGZSYZMD low-dose; [d]$P<0.05$, [dd]$P<0.01$ vs. JWGZSYZMD medium-dose. JWGZSYZMD, Jiawei Guizhishaoyaozhimu Decoction; CIA, collagen II-induced arthritis; Q, quartile.

Table V. Primers for reverse transcription-quantitative PCR analysis.

Gene target	Sequence (5'-3')
IL-1β	F: CTCTGTGACTCGTGGGATGATG
	R: CACTTGTTGGCTTATGTTCTGTCC
IL-6	F: AACGAAAGTCAACTCCATCTG
	R: GGTATCCTCTGTGAAGTCTCC
TNF-α	F: TGGCCCAGACCCTCACACTC
	R: CTCCTGGTATGAAATGGCAAATC
IL-17A	F: ACAGTGAAGGCAGCGGTACT
	R: GCTCATAGTCCAGGGTGAAG
β-actin	F: CACCCGCGAGTACAACCTTC
	R: CCCATACCCACCATCACACC

F, forward; R, reverse.

Discussion

RA is a heterogeneous, systemic and chronic autoimmune disease that is characterized by the non-infectious inflammation of joints and periarticular tissues (28,29). The majority of patients with RA also have extra-articular multisystem involvement, which can further aggravate the condition (28,29). An effective, integrated Traditional Chinese and Western medicinal treatment that can alleviate the inflammation whilst also preventing bone destruction is necessary for treatment of this disease. If the body is weak, or feels seasonal changes, it may cause this disease, RA has been previously attributed by the TCM research field to 'arthralgia syndrome', where this disease is called 'Wang Bi' (30). As this condition is recalcitrant, protracted and refractory and pain traverses the characteristics of multiple joints throughout the body, it is also considered to be different from general arthralgia syndrome (30). RA is typically classified as a special type of arthralgia syndrome, which is similar to 'Li Jie', a different joint disease, mentioned in the 'Synopsis of the Golden Chamber - Concurrent Treatment of Stroke Syndrome' (31). According to the aforementioned synopsis, RA is 'a disease involving multiple joints, making them unable to flex or extend', 'swollen, painful joints with limited function'. The Guizhi Shaoyao Zhimu decoction was set by Zhang Zhongjing, a doctor of TCM, for rheumatism affecting multiple joints. This medicine contained nine components and is a common prescription in China for treating RA (1-3).

The main manifestations of RA are the symmetrical polyarthritis of the joints, including hands, wrists and feet, although it can also involve joints in the knees and hips. RA can also exhibit a number of extra-articular manifestations. Among its joint manifestations, swelling and deformation are common symptoms (32). The inflammatory response induced by the CIA model used in the present study was reported to induce polyperipheral arthritis, mainly in the feet, ankle and knee joints, which causes local redness, swelling and deformity of the joints (33). Pathological manifestations include proliferative synovitis, articular cartilage destruction, bone

erosion, pannus formation and inflammatory cell infiltration. The clinical manifestations, laboratory parameters and immune and pathological changes are similar to those of human RA (34). Therefore, using the CIA rat model, the therapeutic effects of the drug on joint inflammation were assessed by drug intervention followed by the regular observation of changes in the joints of the rats. A number of studies have reported the treatment of clinical RA with Guizhi Shaoyao Zhimu Decoction (12,13,35), however, to the best of our knowledge, there are currently no reports on its mechanism of action, which limits the application of this treatment for RA.

In the present study, the network relationship of 'drug-active ingredient-disease target' was constructed through the network pharmacology, where the potential active ingredients contained within JWGZSYZMD for the treatment of RA were analyzed. Among those list were quercetin, angelicin, kaempferol, 7-methoxy-2-methyl isoflavone, naringin, formononetin, isorhamnetin, icaritin, alfalfa toxin and stigmasterol. Quercetin is a subclass of flavonoids with reported anti-inflammatory and antioxidant effects (36,37). Hashemi *et al* (38) previously reported that quercetin could reduce the production of inflammatory cytokines and IL-17 by inhibiting the Toll-like receptor 4/MAPK signaling pathway, thereby reducing the polarization of T helper 17 (Th17) cells and inhibiting the inflammatory response. In addition, core targets of JWGZSYZMD found in the therapy of RA in the present study include AKT1, TNF, IL-6, VEGFA and IL-1B, following analysis of the PPI network. These aforementioned core targets also underwent KEGG pathway enrichment analysis. The KEGG results indicated that the core targets were mainly enriched in inflammatory related pathways, such as IL-17, TNF, PI3K/Akt and MAPK. During RA synovial inflammation, MAPK signaling forms one of the core mechanisms mediating the occurrence of inflammation. MAPK signaling in synovial cells is mainly activated by TNF-α and IL-1, resulting in the production of cytokines to promote the inflammatory response (39,40). The major family members of MAPK signaling include p38 MAPK, ERK1/2 and JNK, all of which are present in phosphorylated forms in synovial tissue of RA patients. (41). Another study previously reported that p38 MAPK can regulate IL-17 signaling upstream of proinflammatory and mediator cytokines (42).

In the present study, the joint scores of the model group were increased after collagen II treatment, whilst those in the JWGZSYZMD treatment groups were decreased compared with those in the model group after collagen II treatment. In terms of pathology, the synovium in the CIA model group exhibited notable inflammatory cell infiltration, where the cartilage showed synovial erosion. By contrast, the degree of synovial inflammatory cell infiltration and cartilage erosion in the low- and medium-dose groups of JWGZSYZMD were markedly milder compared with those in the CIA model group. In addition, only a small quantity of inflammatory cells could be observed in the high-dose group of JWGZSYZMD. The pathophysiological features after JWGZSYZMD treatment were found to be alleviated at a high-dose compared with those in the model group. A similar result was observed with the tripterygium glycoside treatment group. This suggests that this decoction can relieve joint swelling and deformation in the CIA model animals, even though there were no significant

differences in joint scores between dose groups. The results of the present study could be influenced by the small sample of rats in each group. However, high-doses of JWGZSYZMD decreased the expression of IL-1β, IL-6, IL-17 and TNF-α in the synovium of model animals, which suggests that this treatment could serve a role in relieving joint inflammation by controlling expression of these factors. IL-1β is one of the most extensively studied subtypes of IL-1β, which is a typical proinflammatory cytokine. It is mainly produced by inflammatory and immune cells and serves an important role in the inflammatory response, bone resorption and cartilage destruction. A previous study reported that IL-1β can serve a positive feedback role in the regulation of NF-κB activation through a series of cascade reactions to aggravate RA (43). IL-1β, after being secreted by the synovial tissue, can activate osteoclasts and chondrocytes to induce bone destruction and cartilage destruction or promote Th17 cell differentiation, which facilitate the pathogenesis of RA (44). TNF-α is produced by activated macrophages, monocytes and T lymphocytes, which can inhibit the synthesis of bone collagen, stimulate the production of prostaglandins and collagenases by fibroblasts and chondrocytes. This in turn stimulates the secretion of MMPs by chondrocytes and induces the differentiation of peripheral blood mononuclear cells into osteoclasts, leading to cartilage destruction, aggravation of the inflammatory response and, consequently, RA pathogenesis (45-47). IL-17A is a cytokine produced by CD4⁺Th17 cells and γδ T cells, which can not only sustain the malignant inflammatory cycle of the joint tissue to promote the occurrence and development of RA but can also promote the production of TNF-α by infiltrating leukocytes (48). The combination of these two processes can cooperatively activate synovial fibroblasts to produce IL-6 (48). IL-6 is a key factor in the pathogenesis of RA, contributing to the production of IgM and IgG rheumatoid factors and citrullinated peptide antibodies, which promote the development of synovitis and joint destruction (49,50).

Previous research has reported that GSZD can reduce the levels of pro-inflammatory factors TNF-α, IL-1β, IL-17 and receptor activator for NF-κB ligand (RANKL), thus inhibiting the recruitment and differentiation of osteoclast precursors. GSZD may also increase the secretion of osteoclastogenesis inhibitory factor (OPG), thereby regulating the ratio of RANKL/OPG that could promote the protection of bone to improve the injury of cartilage and synovium in CIA rats (51). In the present study, 'Gu Sui Bu' (Rhizoma Drynariae), 'Bu Gu Zhi' (Fructus Psoraleae) and 'Sang Zhi' (Ramulus Mori) were added to the original medicinal preparation. Previous studies have reported that these components also serve a positive role in the protection of bone destruction in RA. Bavachinin (derived from 'Bu Gu Zhi') may inhibit the proliferation and migration of MH7A cells and production of inflammatory factors and apoptosis by acting on the PI3K/AKT signaling pathway (52). In addition, 'Gu Sui Bu' flavones can significantly inhibit the loss of bone mass around the inflammatory joints of CIA rats, which can promote bone reconstruction (53). Low dose 'Sang Zhi' could inhibit the expression of the HIF-1α/VEGF/MMP signaling pathway, thereby reducing the inflammatory response and neovascularization of toes in rats, which inhibited the destruction of bone and cartilage (54). The new Chinese medicine presented in the present study was

shown to protect the joints and enhances the curative effect of the original preparation. Therefore, future studies will focus on analyzing the mechanisms related to bone destruction and protection of cartilage.

Results from the present study demonstrated that JWGZSYZMD reduced the expression levels of IL-1β, IL-6, IL-17 and TNF-α in synovium of rats with CIA, which suggests that this treatment may potentially alleviate joint inflammation by inhibiting or downregulating the expression of these inflammatory factors. A wide array of potential active ingredients contained within JWGZSYZMD could bind to core factors involved in RA, such as TNF and IL-6, which may explain the potential therapeutic characteristics of this treatment. The main tools used for studying the molecular docking of chemical components to targets were online databases, therefore, there are some limitations associated with these methods, such as the delayed updates of databases and incomplete inclusion degrees. Further verification should be performed on the basis of continuous updates associated with these databases. Future research should aim to clarify the specific mechanism of action of JWGZSYZMD for the treatment of RA to provide a more precise theoretical basis for the clinical treatment of RA. For example, future experiments could compare the efficacy of glycyrol, eriodictyol and diosgenin for the treatment of RA.

Acknowledgements

Not applicable.

Funding

Availability of data and materials

The datasets used and/or analyzed during the current study are available from the corresponding author on reasonable request.

Authors' contributions

YC and WJ designed the study, performed the experiments and wrote the paper. YJ and KF analyzed data. XZ and YX calibrated the data and revised the paper. All authors read and approved the final version of the manuscript. YC and WJ confirm the authenticity of all the raw data.

Ethics approval and consent to participate

The present study was approved by the Medical and Experimental Animal Ethics Committee of The Beijing University of Traditional Chinese Medicine (approval no. BU CM-4-2021090605-3104).

Patient consent for publication

Not applicable.

Competing interests

The authors declare that they have no competing interests.

References

1. Zheng AP and Zheng XH: Evolution and information analysis of classical formulas Guizhi Shaoyao Zhimutang. Chinese J Experimental Traditional Medical Formulae 29: 174-184, 2023.
2. Daily JW, Zhang T, Cao S and Park S: Efficacy and safety of GuiZhi-ShaoYao-ZhiMu decoction for treating rheumatoid arthritis: A systematic review and meta-analysis of randomized clinical trials. J Altern Complement Med 23: 756-770, 2017.
3. Yuan N: Effect of GuizhiShaoyaoZhimu Decoction on rheumatoid arthritis. Cardiovascular Disease. J Integr Trad Chin Western Med 6: 163-164, 2018 (In Chinese).
4. Chinese Rheumatology Association: 2018 Chinese guideline for the diagnosis and treatment of rheumatoid arthritis. Chin J Intern Med 57: 242-251, 2018.
5. England BR, Thiele GM, Anderson DR and Mikuls TR: Increased cardiovascular risk in rheumatoid arthritis: Mechanisms and implications. BMJ 361: k1036, 2018.
6. Liu W, Fan Y, Tian C, Jin Y, Du S, Zeng P and Wang A: Deciphering the molecular targets and mechanisms of HGWD in the treatment of rheumatoid arthritis via network pharmacology and molecular docking. Evid Based Complement Alternat Med 2020: 7151634, 2020.
7. Huang J, Fu X, Chen X, Li Z, Huang Y and Liang C: Promising therapeutic targets for treatment of rheumatoid arthritis. Front Immunol 12: 686155, 2021.
8. Bradfield PF, Amft N, Vernon-Wilson E, Exley AE, Parsonage G, Rainger GE, Nash GB, Thomas AM, Simmons DL, Salmon M and Buckley CD: Rheumatoid fibroblast-like synoviocytes over-express the chemokine stromal cell-derived factor 1(CXCL12), which supports distinct patterns and rates of CD4+and CD8+T cell migration within synovial tissue. Arthritis Rheum 48: 2472-2482, 2003.
9. Filer A, Parsonage G, Smith E, Osborne C, Thomas AMC, Curnow SJ, Ed Rainger G, Raza K, Nash GB, Lord J, *et al*: Differential survival of leukocyte subsets mediated by synovial, bone marrow, and skin fibroblasts:Site-specific versus activation-depend-ent survival of T cells and neutrophils. Arthritis Rheum 54: 2096-2108, 2006.
10. Zheng DN, Hu LF, Kong WP and Yan XP: An analysis of Professor Yan Xiaoping's experience in treating rheumatoid arthritis by tonifying the kidney and strengthening the bones. J China-Japan Friendship Hospital 34: 116-118, 2020 (In Chinese).
11. Xu Y, *et al*: Effects of kidney-supplementing cold-dispelling Zhi Wang Tang decoction on inflammation, bone erosion and Wnt/β-catenin pathway in rats with colla-gen-induced arthritis, 2020, 43(04), 289-295.
12. Jing WX, Yan XP. YAN Xiao-ping's experience in the diagnosis and treatment of rheumatism discussing by 'combine and harmony'. China Journal of Traditional Chinese Medicine and Pharmacy, 2021, 36(8):4.
13. Wang WR, Shi LC, Liu S, *et al*: Professor YAN Xiaoping's experience in treating zhoubi(palindromic rheumatism). Tianjin Journal of Traditional Chinese Medicine 2021, 38(12): 1505-1508.
14. Guo W, Huang J, Wang N, Tan HY, Cheung F, Chen F and Feng Y: Integrating Network pharmacology and pharmacological evaluation for deciphering the action mechanism of herbal formula Zuojin Pill in suppressing hepatocellular carcinoma. Front Pharmacol 10: 1185, 2019.
15. LiHL,ChenC and ChenC:Network pharmacology-based approach to investigate the mechanism of Huang-Lian-Jie-Du-Decoction for treatment of type 2 diabetes mellitus. Traditional Medicine Research 6: 36, 2021.
16. Li D, Fan H, Dong J, Sun C, Su Y, Liu J and Gu Y: Based on BATMAN-TCM to explore the molecular mechanism of Xihuang Pill regulating immune function to treat breast precancerous lesions. Breast Cancer (Dove Med Press) 13: 725-742, 2021.
17. Zhang J, Zhou Y and Ma Z: Multi-target mechanism of Tripteryguim wilfordii Hook for treatment of ankylosing spondylitis based on network pharmacology and molecular docking. Ann Med 53: 1090-1098, 2021.

18. Szklarczyk D, Gable AL, Lyon D, Junge A, Wyder S, Huerta-Cepas J, Simonovic M, Doncheva NT, Morris JH, Bork P, et al: STRING v11: Protein-protein association networks with increased coverage, supporting functional discovery in genome-wide experimental datasets. Nucleic Acids Res 47(D1): D607-D613, 2019.
19. Chen L, Zhang YH, Lu G, Huang T and Cai YD: Analysis of cancer-related lncRNAs using gene ontology and KEGG paths. Artif Intell Med 76: 27-36, 2017.
20. Kondo N, Kuroda T and Kobayashi D: Cytokine networks in the pathogenesis of rheumatoid arthritis. Int J Mol Sci 22: 10922, 2021.
21. Takeuchi T, Yoshida H and Tanaka S: Role of interleukin-6 in bone destruction and bone repair in rheumatoid arthritis. Autoimmun Rev 20: 102884, 2021.
22. Xu SY, Bian R and Chen X: Experimental methodology of pharmacology. People's Medical Publishing House, 2002.
23. Ding Y, Ma T and Yang XQ: Effects of high dose glycosides of Tripterygium wilfordii Hook. f on the fertility of young rats. Zhongguo Zhong Xi Yi Jie He Za Zhi 32: 61-63, 2012 (In Chinese).
24. Liu C, He L, Wang J, Wang Q, Sun C, Li Y, Jia K, Wang J, Xu T, Ming R, et al: Anti-angiogenic effect of Shikonin in rheumatoid arthritis by downregulating PI3K/AKT and MAPKs signal paths. J Ethnopharmacol 260: 113039, 2020.
25. Livak KJ and Schmittgen TD: Analysis of relative gene expression data using real-time quantitative PCR and the 2(-Delta Delta C(T)) method. Methods 25: 402-408, 2001.
26. Lu JD, Ge XY, Wang HL, et al: Effect of Guizhi Shaoyao Zhimu Decoction combined with Methotrexate in the treatment of cold-damp blockage syndrome of rheumatoid arthritis. China Medical Herald,2021,8(18):4.
27. Hsin KY, Ghosh S and Kitano H: Combining machine learning systems and multiple docking simulation packages to improve docking prediction reliability for network pharmacology. PLoS One 8: e83922, 2013.
28. Wang Z, Huang J, Xie D, He D, Lu A and Liang C: Toward overcoming treatment failure in rheumatoid arthritis. Front Immunol 12: 755844, 2021.
29. Liu L, Wang D, Liu MY, Yu H, Chen Q, Wu Y, Bao R, Zhang Y and Wang T: The development from hyperuricemia to gout: Key mechanisms and natural products for treatment. Acupunct Herb Med 2: 25-32, 2022.
30. Jiao SD and Wang WG: Study on Disease Name Wangbi and Its Treatment Discipline. J Zhejiang Chin Med Univ 33: 5, 2009.
31. Sun Y, Ma WQ, Qu XP, .Implications of Gui Zhi Pao Yao Zhi Materia Medica Soup in 'The Essentials of the Golden Chamber' for the treatment of rheumatoid arthritis by the method of 'Supporting Positive and Dispelling Evil'. Global Traditional Chinese Medicine, 2019, 12(3), 427-429.
32. Fraenkel L, Bathon JM, England BR, St Clair EW, Arayssi T, Carandang K, Deane KD, Genovese M, Huston KK, Kerr G, et al: 2021 American college of rheumatology guideline for the treatment of rheumatoid arthritis. Arthritis Care Res (Hoboken) 73: 924-939, 2021.
33. Harris HE, Liljeström M and Klareskog L: Characteristics of synovial fluid effusion in collagen-induced arthritis (CIA) in the DA rat; a comparison of histology and antibody reactivities in an experimental chronic arthritis model and rheumatoid arthritis (RA). Clin Exp Immunol 107: 480-484, 1997.
34. Kim YH and Kang JS: Effect of methotrexate on collagen-induced arthritis assessed by micro-computed tomography and histo-pathological examination in female rats. Biomol Ther (Seoul) 23: 195-200, 2015.
35. Liu ZD and Shi LP: Effect of Jiawei Guizhishaoyaozhimu Decoction on ESR, CRP and RF in Patients with Active Rheumatoid Arthritis, Shaanxi J Trad Chin Med 40: 82-84, 2019 (In Chinese).
36. Singh P, Arif Y, Bajguz A and Hayat S: The role of quercetin in plants. Plant Physiol Biochem 166: 10-19, 2021.
37. Marunaka Y, Marunaka R, Sun H, Yamamoto T, Kanamura N, Inui T and Taruno A: Actions of quercetin, a polyphenol, on blood pressure. Molecules 22: 209, 2017.
38. Hashemi AM, Kahnamouii SS, Aghajani H, Frozannia K, Pournasrollah A, Sadegh R, Esmaeeli H, Ghadimi Y and Razmpa E: Quercetin decreases Th17 production by down-regulation of MAPK-TLR4 signaling path on T cells in dental pulpitis. J Dent (Shiraz) 19: 259-264, 2018.
39. Xu ZH, Li X, Lin Y, et al: Guizhi Shaoyao Zhimu decoction combined with methotrexate in the treatment of rheumatoid arthritis: A meta-analysis. Hunan Journal of Traditional Chinese Medicine,2020,36(8):5.
40. Gao F, Bao SY and Fu Q: Research progress of traditional Chinese medicine regulating MAPK signal path in the treatment of rheumatoid arthritis. Information on Traditional Chinese Medicine. 2022, 39 (1):75-79, ISTIC, 2022:Inner Mongolia Autonomous Region Science and Technology Planning project.
41. Lu M, Wang Y and Zhan X: The MAPK pathway-based drug therapeutic targets in pituitary adenomas. Front Endocrinol (Lausanne) 10: 330, 2019.
42. Liu S, Ma H, Zhang H, Deng C and Xin P: Recent advances on signaling pathways and their inhibitors in rheumatoid arthritis. Clin Immunol 230: 108793, 2021.
43. Shi YJ anf Shen J: Effect of Guizhi Shaoyao Zhimu Decoction on Serum Inflammatory Factors, OPG and RANKL Levels in Patients with Rheumatoid Arthritis of Wind-cold-dampness Arthralgia Type. J Sichuan Trad Chin Med 36: 106-109, 2018 (In Chinese).
44. Zeng Q, Wang CF and Zhu H: Treating 96 cases of rheumatoid arthritis with the Guizhi Shaoyao Zhimu decoction. Clin J Chin Med 10: 77-78, 2018 (In Chinese).
45. Carter SD, Barnes A and Gilmore WH: Canine rheumatoid arthritis and inflammatory cytokines. Vet Immunol Immunopathol 69: 201-214, 1999.
46. Murakami T, Nakaminami Y, Takahata Y, Hata K and Nishimura R: Activation and function of NLRP3 inflammasome in bone and joint-related diseases. Int J Mol Sci 23: 5365, 2022.
47. Slowikowski K, Nguyen HN, Noss EH, Simmons DP, Mizoguchi F, Watts GFM, Gurish MF, Brenner MB and Raychaudhuri S: CUX1 and IκBζ (NFKBIZ) mediate the synergistic inflammatory response to TNF and IL-17A in stromal fibroblasts. Proc Natl Acad Sci USA 117: 5532-5541, 2020.
48. Shi H, Wang DT, Wu RG, et al: Role of TNF-α-mediated NF-κB signal path in angiogenesis of rheumatoid arthritis. Medical Recapitulate, 2012,18(15):2397-2400.
49. Chen HM and Wang YL: Role and regulation of osteoclasts in the pathological changes of bone destruction caused by rheumatoid arthritis. Chin J Osteop 22: 6, 2016 (In Chinese).
50. Yuan S, Li X, Lin A and Larsson SC: Interleukins and rheumatoid arthritis: Bi-directional Mendelian randomization investigation. Semin Arthritis Rheum 53: 151958, 2022.
51. Shujun W: Experimental Study on Bone Protective Effect and Mechanism of Guizhi-Shaoyao-Zhimu Decoction in Rheumatoid Arthritis (unpublished PhD thesis). Chengdu University of Traditional Chinese Medical, 2022.
52. Deng H, Jiang J, Shu J, Huang M, Zhang QL, Wu LJ and Sun WK: Bavachinin ameliorates rheumatoid arthritis inflammation via PPARG/PI3K/AKT signaling pathway. Inflammation 46: 1981-1996, 2023.
53. Xiaojun G, Jun X, Lianbo X, Chao L, Huali G, Xinxing H, Ningli L and Danjun MA: Therapeutic effect of drynaria total flavonoids on the bone destruction of CIA rat. Journal of Clinical Medicine in Practice 17: 13-17, 2013.
54. Qing D, Fei H, DQingqiao H, et al: Study of Ramulus Mori on bone destruction in adjuvant-induced arthritis rats by regulating HIF-1α/VEGF/MMPs signaling pathway. Journal of Hunan University of Chinese Medicine 42: 1096-1104, 2022.